International Immunopharmacology 76 (2019) 105899

Contents lists available at ScienceDirect

International Immunopharmacology

journal homepage: www.elsevier.com/locate/intimp

Novel pharmacological inhibition of EZH2 attenuates septic shock by altering innate inflammatory responses to sepsis

Qianqian Zhang[a,1], Hong Sun[b,1], Shougang Zhuang[c,d], Na Liu[c], Xiaowei Bao[b], Xiandong Liu[b], Huijuan Ren[b], Diyu Lv[b], Zhe Li[a], Jianwen Bai[b], Xiaohui Zhou[e,*], Lunxian Tang[b,f,**]

[a] Medical School/Tongji University, Shanghai 200120, China
[b] Department of Internal Emergency Medicine and Critical Care, Shanghai East Hospital, Tong Ji University, Shanghai 200120, China
[c] Department of Nephrology, Shanghai East Hospital, Tongji University School of Medicine, Shanghai, China
[d] Department of Medicine, Rhode Island Hospital and Alpert Medical School, Brown University, Providence, RI, USA
[e] Research Center for Translational Medicine, Shanghai East Hospital, Tongji University, Shanghai 200120, China
[f] Department of Internal Emergency Medicine and Critical Care, ji'an Hospital, Shanghai East Hospital, ji'an, jiangxi, China

ARTICLE INFO

Keywords:
EZH2
Innate immunity
Sepsis

ABSTRACT

The function of histone methyltransferase enhancer of zeste homolog 2 (EZH2) in sepsis remains unknown. We reported here that the expression of EZH2 and H3K27me3 was significantly upregulated in the circulation of septic patients, whereas patients who survived presented downregulated the expression of EZH2 on CD14+ monocytes. We further identified increased expression of EZH2 in the circulation, peritoneal fluid, and septic lungs from CLP mice. 3-DZNeP treated CLP mice improved mortality and protected from organ injury. EZH2 inhibition not only suppressed the activation of inflammatory cells and release of cytokines in the circulation and infectious sites, but also promoted bacteria clearance and replenished the circulating monocyte and neutrophil pool from bone marrow. Blockage of EZH2 also suppressed the progression of lung injury and alleviated inflammation by decreasing the pulmonary cell apoptosis, reducing inflammatory cells infiltration and cytokines release through inhibition of the STAT3 signaling pathway and recovery of PPARγ activation. In addition, EZH2 inhibitor blunted macrophage M1 polarization by SOCS3/STAT1 pathway. Overall, these data suggest that EZH2 could be a potential biomarker predicting clinical outcome and a new target for therapeutic interference in sepsis.

1. Introduction

Sepsis and septic shock are progressive, inflammatory responses to overwhelming infections associated with tissue hypoperfusion and multiorgan dysfunction [1,2], which are still the leading causes of death in critically ill patients in the world, and all pharmacological treatments and clinical trials have so far failed to show efficacy. The World Health Organization has declared sepsis a global health priority by adopting a resolution to improve the prevention, diagnosis and management of this deadly disease [2].

Epigenetic changes are well known to play critical roles in the inflammatory responses seen during sepsis [3]. Extensive reports have documented that DNA methylation/demethylation and histone deacetylation/acetylation as two main epigenetic events could be the important epigenetic modifiers in reducing inflammation-related pathologies during sepsis [4]. However, studies examining the efficacy of histone methylation in modulating cytokines and macrophages to quench inflammation and prevent mortality during sepsis are still scarce.

Histone methylation is an essential epigenetic mechanism that regulates transcription and chromatin dynamics, and has roles in pathogenic development and the maintenance of normal physiology [5].

Abbreviations: EZH2, histone methyltransferase enhancer of zeste homolog 2; HMTs, histone lysine methyltransferases; H3K27me3, histone H3 at lysine 27; PRC2, polycomb repressive complex 2; 3-DZNeP, 3-deazaneplanocin A; CLP, cecal ligation and puncture; TNF-α, tumor necrosis factor-α; MIP-2, macrophage inflammatory protein-2

* Correspondence to: X. Zhou, Research Center for Translational Medicine, Shanghai East Hospital, Tongji University, 150, Jimo Road, Shanghai 200120, China.
** Correspondence to: L. Tang, Department of Internal Emergency Medicine and Critical Care, Shanghai East Hospital (South), Tongji University, 1800, Yuntai Road, Shanghai 200120, China.
E-mail addresses: xhzhou100@126.com (X. Zhou), lunxiantang@hotmail.com (L. Tang).
[1] These authors contributed equally to this work.

https://doi.org/10.1016/j.intimp.2019.105899
Received 26 June 2019; Received in revised form 6 August 2019; Accepted 6 September 2019
Available online 10 September 2019

Methylation occurs on lysine and arginine residues of histone proteins [6]. This process is regulated by histone lysine methyltransferases (HMTs) and demethylases (HDMs). Studies have revealed that the process of inflammation and infection in inflammatory cells is regulated by histone methylation, including H3K4, H3K9, and H3K27 methylation [7,8]. Histone H3 at lysine 27 (H3K27me3) is a transcriptionally repressive epigenetic marker that has been associated with suppression of multiple tumor suppressor genes. Enhancer of zeste homolog 2 (EZH2) is the catalytic component of a multi-protein complex, polycomb repressive complex 2 (PRC2) [9]. PRC2 catalyzes the trimethylation of H3K27me3. EZH2 is found to be positively associated with poor clinical outcomes in many aggressive tumors [9]. Studies have also shown that EZH2 is highly upregulated in the fibrotic tissues of lung, kidney, and liver. Furthermore, 3-deazaneplanocin A (3-DZNeP), a carbocyclic analog of adenosine, can also inhibit H3K27me3 by depletion of cellular level of EZH2 [9,10]. Currently, this compound is widely used in preclinical and in vitro studies to investigate the function of EZH2 in cancer and fibrotic diseases, and has been shown to effectively inhibit cell proliferation and prevent tumor progression [11]. A recent study has documented that pharmacological ablation with EZH2/let-7c/PAK1 signal results in resistance to LPS-induced endotoxin shock via blunting macrophage M1 polarization [12]. A more recent recently has reported that overexpression of EZH2 is found in the heart of sepsis rat [13]. However, changes of EZH2 and H3K27me3 in the circulation of patients with critical illness and sepsis have not been explored. Furthermore, it is not clear what the roles of EZH2 are to septic inflammatory responses, and whether targeting the suppression of EZH2 can attenuate the overwhelming innate inflammatory responses seen during sepsis.

This study examined the role of EZH2 in innate immune responses in septic shock.

2. Materials and methods

2.1. Patients

Peripheral blood was collected from identified patients in the Intensive Care Unit of East Hospital. The mononuclear ring was collected after Ficoll hypaque gradient centrifugation. The cells were purified and then processed for EZH2 expression via western-blotting and H3K27me3 expression via EpiQuik Global Tri-Methyl Histone H3K27 Quantification Kit as the manufacture recommended. Investigators were blinded to the clinical data. A total of 20 eligible patients were classified as sepsis and septic shock according to the clinical criteria for sepsis-3. The patients were followed by 28 days and divided into survival and non-survival groups according to whether they were alive or not. For comparison, peripheral blood was also taken from healthy volunteers who came to East hospital for routine physical examination. The study was approved by the Research Ethics Board of East Hospital, Tongji University (Shanghai, China). Written informed consent was obtained from all recruited patients or their authorized family members.

2.2. Mice

Male C57BL/6 mice aged 6–8 weeks (16–18 g) were purchased from *Shanghai* Jie Si Jie *Lab Animal* Co. Ltd. (Shanghai, China) and housed in a pathogen-free facility at Tongji University. All animal experiments were performed according to the guidelines for the Care and Use of Laboratory Animals (Ministry of Health, China, 1998). Experiments were conducted under protocols approved by the Animal Use Committee of East Hospital/Tongji University.

2.3. Cecal ligation and puncture (CLP) and experimental design

CLP-Mice were anesthetized using Isoflurane. A midline incision (~1 cm) was made below the diaphragm, exposing the cecum, and then the cecum was ligated distally and punctured twice with a 22-gauge needle. In the control animals (sham), the cecum was located and mobilized but was neither ligated nor punctured. The abdominal incision was then closed in layers with an Ethilon 6.0 suture, and the animals were resuscitated with 1.0 ml lactated Ringer's solution by subcutaneous injection as previously reported [14].

To assess whether pharmacological inhibition of EZH2 with 3-DZNeP could protect the mice from CLP-induced septic shock, we tested different doses of 3-DZNeP (1, 2, and 5 mg/kg) and two different administering time (1 h post-CLP vs. 24 h before followed by 1 h after CLP). We found that administration of 3-DZNeP at 2 mg/kg (i.p.) twice prolonged the time to death (data not shown). Based on this result, In the survival experiment, mice received intra-peritoneal 3-DZnep [purchased from Selleckchem (Houston, TX)] dissolved in DMSO (50 mg/kg) or vehicle DMSO 24 h before and 1 h after CLP (n = 10/group). The control group of animals was injected with vehicle DMSO only. Mortality was recorded for up to 10 days post-procedure.

In the non-survival experiment, animals were randomly assigned to the following three groups (n = 12/group): (a) Sham-operated animals (Sham); (b) Vehicle treated CLP animals received intra-peritoneal vehicle DMSO 24 h before and 1 h after CLP (CLP + DMSO), and (c) 3-DZnep treated animals received intra-peritoneal 3-DZnep dissolved in DMSO (50 mg/kg) 24 h before and 1 h after CLP (CLP + 3-DZnep). At the time of sacrifice [24 h/48 h after CLP], abdominal cavity was opened and irrigated with 1 ml normal saline, which was collected for analysis, and blood samples were collected by cardiac puncture. Lung tissue, peritoneal fluid, bone marrow, spleen, liver, jejunum and heart samples were harvested 24 h after CLP, whereas samples were collected 48 h after CLP for histological analysis, which were fixed in 10% buffered formalin as previously reported [15].

2.4. Evaluation of systemic and local bacterial burden

Blood samples were collected and spread on Trypticase Soy Agar with 5% Sheep Blood (TSA II) agar plate (BD Bioscicence) with dilutions of 1 μl, 10 μl or 100 μl in 100 μl saline aliquots. Peritoneal lavage fluid was harvested after injecting 2 ml of PBS into the peritoneum and serially diluted in sterile saline. A 100 μl aliquot of each dilution was spread on a TSA II blood agar plate. All plates were incubated at 37 °C for 24–48 h. Colonies were counted and expressed as CFU/100 μl for blood samples or CFU/ml for peritoneal lavage samples.

2.5. Cytokines and chemokine measurements

Concentrations of tumor necrosis factor-α (TNF-α), interleukin-6, interferon-γ (IFN-γ), IL-1β, IL-4, KC and macrophage inflammatory protein-2 (MIP-2) in the peritoneal fluid, plasma or lung tissue homogenates were measured using the Quantikine Enzyme-Linked Immunosorbent Assay (ELISA) Kit (R&D Systems, Minneapolis, MN) according to manufacturer's instructions.

2.6. Peritoneal macrophage isolation and phagocytosis assay

Peritoneal lavages were performed using 10 ml of PBS. Lavages containing peritoneal exudate cells from individual mice were processed separately. Cells were plated in 6-well tissue culture plates at 4×10^6/ml and incubated in complete RPMI 1640 medium supplemented with 20% heat-inactivated fetal bovine serum (FBS) at 37 °C. Ninety minutes later, non-adherent cells were washed off with PBS. Adherent macrophages were isolated. Macrophage phagocytic activity was measured using the Vybrant Phagocytosis Assay Kit (Invitrogen). Cells were further incubated with heat-inactivated, fluorescein-labeled *Escherichia coli* K-12 BioParticles for 2 h, after which extracellular fluorescence was quenched by trypan blue and phagocytic activity was quantified by measuring fluorescence intensity of the uptaken particles

emission at 520 nm with an excitation at 485 nm using a microplate reader (SpectraMax M5). The negative controls were prepared by adding vehicles and fluorescence labeled probes without cells; and macrophages of sham mice were used as positive controls. Results were expressed as the percentage of increase compared with positive controls after deduction of negative controls as suggested by the kit instructions. Co-cultured with ~60 μg of pHrodo - conjugated *E. coli* (Life Technologies) in PBS at 37 °C for 1 h and then were washed completely with PBS. Cells were harvested by scraping and detected by flow cytometry. The percentages of pHrodo positive cells were used as indicators of the capacity of phagocytosis.

2.7. Lung histology and immunofluorescence staining

For lung histology, the left upper lobe of the lung was harvested and fixed in 10% formalin, paraffin embedded and tissue sections were prepared as previously described [15]. Samples were then stained with hematoxylin and eosin (H & E) and examined by light microscopy. For immunofluorescent staining, the tissue sections were rehydrated and labeled with antibodies, including primary antibodies F4/80 (1:100), Ly6G (1:100),TUNEL (1:100) and EZH2 (1:100) and then exposed to Texas red-labeled or FITC green-labeled secondary antibodies (Invitrogen).

2.8. MPO activity in lung tissue and wet/dry (W/D) ratio of lung

Lung MPO activity, a marker for neutrophil influx, was measured by using the Fluorometric Activity Assay Kit (Sigma Aldrich, St Louis, MO) as previously described [15].

After anesthetic overdose and exsanguination (by severing of the inferior vena cava and the abdomen aorta), all the excised lung lobes per mouse were weighed (wet weight), placed in an oven, and weighed daily until the weight unchanged (dry weight). The wet/dry weight ratio was then calculated.

2.9. Isolation of lung mononuclear cells

Lung mononuclear cells were isolated as previously described (Liu X., 2018). Briefly, lungs were minced and incubated at 37 °C in an enzyme cocktail of RPMI containing 2.4 mg/ml collagenase I and 20 μg/ml DNase (Invitrogen), and then mashed through a 70-μm nylon cell strainer (BD Falcon). A 23% and 70% bilayer Percoll (Amersham Biosciences) gradient was performed, and the interface was later collected.

2.10. Immunoblot analysis

Immunoblot analysis was conducted as described previously [14]. Briefly, tissue and cell samples were prepared in lysis buffer (Cell Signaling Technology) containing protease inhibitors cocktail (Roche Diagnostic Co., Indianapolis, IN). After homogenization, the lysate was centrifuged and supernatants were collected for immunoblotting analysis. Immunoblotting was performed using phospho-specific antibody to STAT3(Tyr705)(cat # 9145, Cell Signaling Technology, Inc.; Danvers, MA), phospho-specific antibody to STAT1(Tyr701)(cat # 8217, Cell Signaling Technology, Inc.; Danvers, MA), antibody to SOCS3 (L210)(cat # 2932, Cell Signaling Technology, Inc.; Danvers, MA), antibodies to H3K27me3(C36B11) (cat # 9733, Cell Signaling Technology, Inc.; Danvers, MA) and total H3(cat #ab176842, Abcam, Cambridge, UK.); antibody to PPARγ(C26H12)(cat #2435, Cell Signaling Technology, Inc.; Danvers, MA). GAPDH(cat #2118, Cell Signaling Technology, Inc.; Danvers, MA) were blotted as a loading control as indicated. The densitometry analysis of immunoblotting results was conducted using Image J software developed at the National Institute of Health (NIH).

2.11. Real-time PCR (qRT-PCR)

All reagents, primers, and probes were obtained from Applied Biosystems. An actin GAPDH endogenous control was used for normalization. Reverse transcriptase reactions and real-time PCR were performed according to the manufacturer's protocols. All RT reactions, including no-template controls and RT minus controls, were run in triplicate in Veriti 96 Well Thermal Cycle(Applied Biosystems) GeneAmp PCR 9700 Thermocycler (Applied Biosystems). The following primers were used: EZH2 forward: 5′-TCCATGCAACACCCAACACAT-3′, reverse: 5′-GGGTCTGCTACTGTTATTCGGAA′; CD80 forward: 5′-ACCC CCAACATAACTGAGTCT-3′, reverse: 5′-TTCCAACCAAGAGAAGCG AGG-3′; iNOS forward: 5′-AGCATCCCAAGTACGAGTGG-3′, reverse: 5′-GTGCCCATGTACCAACCATT-3′; CD206 forward: 5′-TCATACCGTGT TGAACCTCT-3′, reverse: 5′-ACAATCATTCCGTTCACCAG-3′. Arginase-1 forward: 5′-CATATCTGCCAAAGACATCGT-3′, reverse: 5′-CCAGCTTGT CTACTTCAGTCA-3′. FIZZ1 forward: 5′-CCAATCCAGCTAACTATCCC TCC-3′, reverse: 5′-CCAGTCAACGAGTAAGCACAG-3′. CD163 forward: 5′-CTGGCGGGTGGTGAAAACA-3′, reverse: 5′-CAGCCGTTACTGCACA CTG-3′. Gene expression levels were quantified using the Quantstudio 6 Flex (Applied Biosystems). ABI Prism 7900HT sequence detection system (Applied Biosystems). Relative expression was calculated using the comparative threshold cycle ($2^{-\Delta\Delta ct}$) method.

2.12. Flow cytometry

Cells in lung tissue digests, peripheral blood, bone marrow and peritoneal fluids were prepared as previously described (Tang L et al., 2014,2015,2017; Bai J et al., 2015; Liu X., 2018). Cells were phenotyped in combination of EZH2, F4/80, iNOS, CD14, Ly6G and CD11b expression by flow cytometry (FACS Array; BD Bioscience, Mountain View, Calif). The following monoclonal Abs (mAbs) conjugated to fluorochromes were used: Alexa Fluor 488 labeled anti-EZH2 (clone 11/EZH2) purchased from BD biosciences; PE/Cy7 labeled anti-iNOS (clone CXNFT) purchased from eBioscience; PE/Cy7-labeled anti-CD11b (clone M1/70), PerCP/Cy5.5-labeled anti- granulocyte differentiation antigen 1 (Ly6G) (clone 1A8), PE-labeled anti-F4/80 (clone BM8) Pacific Blue-labeled anti-CD45 (clone 30-F11), APC-labeled anti-Ly6G (clone RB6-8C5), PE/Cy7 anti-CD14 (clone M5E2) were purchased from Biolegend. Antibodies and their isotype controls were used according to the manufacturer's recommendations. Data were collected on a FACS Array flow cytometer (BD Bioscience) and analyzed using FlowJo software (Tree Star, Ashland, Ore).

2.13. Statistical analyses

Data are presented as mean ± SEM, and analyzed using GraphPad Prism 5 statistical analysis and graphing software. Unpaired student *t*-test was used to determine differences between the two groups. Multiple group comparisons were performed using one-way ANOVA with the post hoc test of Tukey's. $P < 0.05$ was considered significant.

3. Results

3.1. The expression of EZH2 and H3K27me3 is upregulated in the circulation of septic patients and those who died present higher frequency of $EZH2^+$ monocytes in the blood

We first examined the expression of EZH2 and H3K27me3 in the circulation of healthy controls and septic patients. EZH2 mRNA level was noticed significantly upregulated in peripheral blood of septic patients versus healthy controls (Fig. 1A). At the protein level, a significant increase in EZH2 expression was also observed in septic patients compared to healthy controls (Fig. 1B).

Since EZH2 trimethylates the histone H3K27, we measured this histone using EpiQuik Global Tri-Methyl Histone H3K27 Quantification

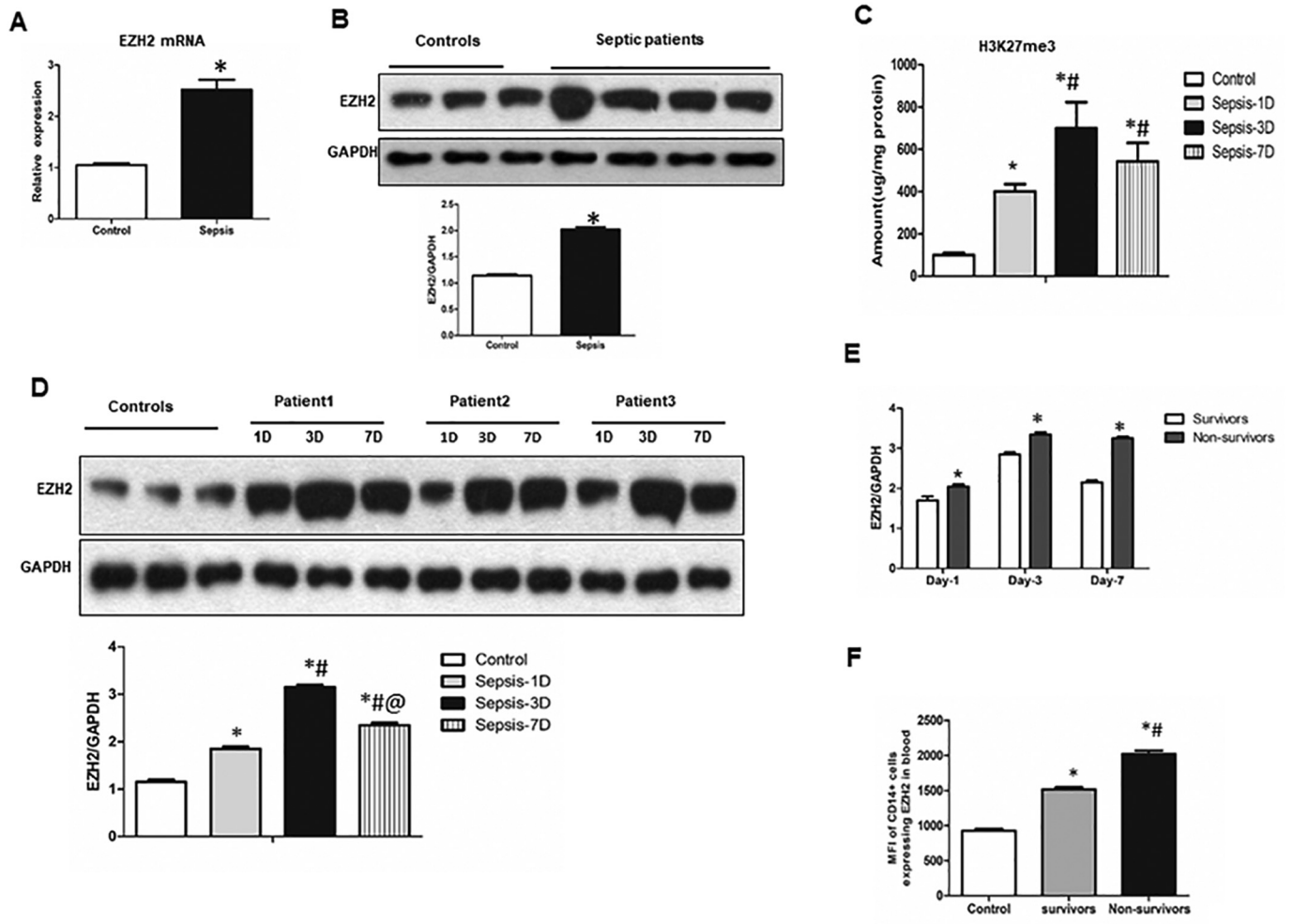

Fig. 1. The expression of EZH2 and H3K27me3 is upregulated in the circulation of septic patients and those who died present higher frequency of EZH2$^+$ monocytes in the blood. (A) The mRNA expression of EZH2 was measured by quantitative PCR on Day 1 in septic patients (N = 20) and healthy controls (N = 10). (B) Representative Western blot depicting mononuclear cell lysates probed for EZH2 and GAPDH from control and septic patients. And Semi-quantitated by densitometry and expressed as integrated density (IDT) values of EZH2 relative to IDT values of GAPDH. All data are expressed as mean ± SEM. (A&B, $^*p < 0.05$ vs. control group, determined by Unpaired student *t*-test). (C) Quantification of H3K27me3 levels in peripheral blood of septic patients on the Day 1, Day 3 and Day 7 post-sepsis and healthy controls. (D) Representative Western blot depicting mononuclear cell lysates probed for EZH2 and GAPDH from control and septic patients on the Day 1, Day 3 and Day 7 post-sepsis. And Semi-quantitated by densitometry and expressed as integrated density (IDT) values of EZH2 relative to IDT values of GAPDH. All data are expressed as mean ± SEM. (C&D, $^*p < 0.05$ vs. control group, $^{\#}p < 0.05$ vs. Day 1 post sepsis, $^{@}p < 0.05$ vs. Day 3 post sepsis determined by one-way ANOVA for multiple group comparisons). (E) The sepsis patients (N = 20) were divided into survivors (N = 14) and Non-survivors (N = 6) according to 28-day clinical outcome. Semi-quantitated of EZH2 was conducted by densitometry and expressed as integrated density (IDT) values of EZH2 relative to IDT values of GAPDH. All data are expressed as mean ± SEM. ($^*p < 0.05$ vs. survivors, determined by Unpaired student *t*-test). (F) The expression of EZH2 on the CD14+ monocytes was assessed by flow cytometry on the first day after diagnosis and the MFI (mean fluorescent intensity) was compared between the survivors and Non-survivors. All data are expressed as mean ± SEM. ($^*p < 0.05$ vs. survivors, determined by Unpaired student *t*-test).

Kit. As shown in Fig. 1C, there was a significant increase in H3K27me3 levels in peripheral blood of septic patients compared to healthy controls, which is consistent with the observed increase in EZH2 level in septic patients. We then assessed serial EZH2 and H3K27me3 expression levels in the peripheral blood of septic patients on Day 1, Day 3, and Day 7 post sepsis. We found that both EZH2 and H3K27me3 levels were significantly increased on Day 3 and Day 7 when comparing with Day 1, while a significant reduction of EZH2 but not H3K27me3 was noted on Day 7 when compared to Day 3 (Fig. 1C, D). Furthermore, expression of EZH2 on CD14$^+$ monocytes in the peripheral blood was assessed and compared between survivors and non-survivors. We observed that those who died were more likely to be older, higher score of severity of illness and underlying physiologic derangement and co-morbidities (SOFA and APACHE II scores). Furthermore, we noticed that the dead patients showed a tendency to remain higher level of EZH2 in the blood till Day 7 (Fig. 1E), and had higher expression of EZH2 on CD14$^+$ monocytes than the patients who survived (Fig. 1F). Therefore, EZH2 may be involved in the progress of sepsis.

3.2. Pharmacological inhibition of EZH2 with 3-DZNeP improves acute septic morbidity and mortality following CLP in mice

Next, we evaluated the role of EZH2 in murine CLP models. As expected, mRNA levels of EZH2 were found to be significantly increased in the blood, lung, spleen, heart and liver (data not shown) in CLP murine model. Therefore, we hypothesized that EZH2 may play a pivotal role in the multiple organ dysfunction and mortality post sepsis. As shown in Fig. 2A, 3-DZNeP -treated animals displayed significantly higher long-term survival compared to the DMSO vehicle group.

The development of multiple organ failure is believed to contribute to septic mortality [1]. To determine whether blockage of EZH2 could lessen the detrimental effects of sepsis on various organ systems, we

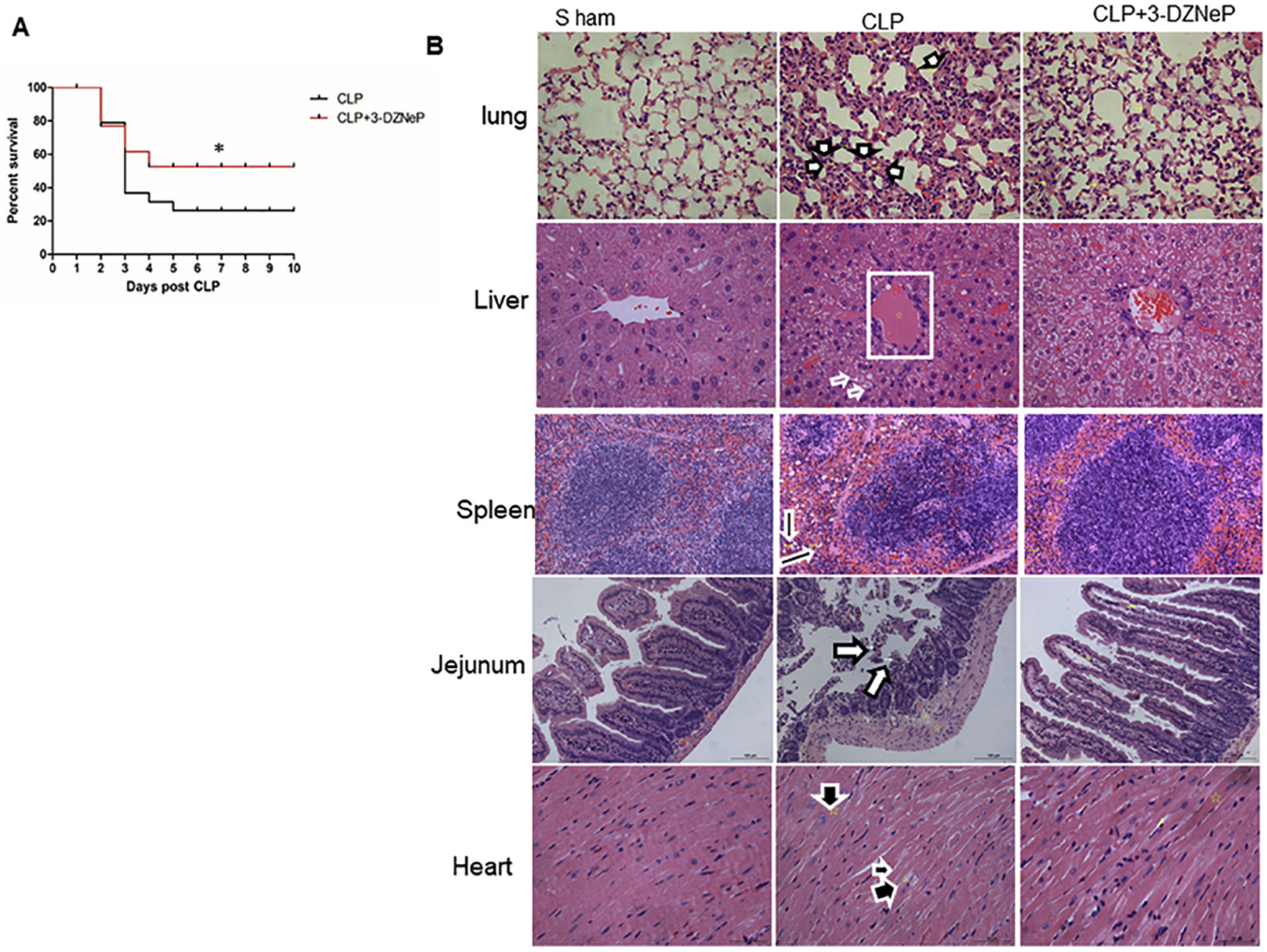

Fig. 2. Pharmacological inhibition of EZH2 with 3-DZNeP improves acute septic morbidity and mortality following experimental sepsis induction (CLP) in mice. (A) CLP surgery was performed on 3-DZNep (N = 15) and DMSO vehicle group (N = 15) mice, and survival was monitored for 10 days. Mice were intraperitoneally administered 3-DZNep at 2 mg/kg or vehicle DMSO 24 h before and 1 h after CLP. Treatment with 3-DZNep significantly improved long-term survival compared to DMSO vehicle group. $*P < 0.05$, Log Rank test for survival study. (B) Septic morbidity: Paraformaldehyde-fixed lungs, livers, spleens, jejunums, hearts were cut and stained with H&E. N = 3–4.

examined the general pathology of several organs 48 h following CLP (Fig. 2B). With respect to the lung injury, while evidence of thickening of the alveolar septum, inflammatory cells infiltration and increased capillary permeability could be seen, these changes were largely absent in 3-DZNeP -treated septic mice which was comparable to the sham mice (Fig. 2B). In the liver, there were marked pathological changes including congested central vein and necrosis that were evaluated at 48 h after CLP. These histological changes were ameliorated by 3-DZNeP (Fig. 2B). Also, we observed marked disrupted tissue architecture and loss of cellularity in the spleen in vehicle treated CLP mice. By contrast, 3-DZNeP -treated septic splenic histology was relatively normal (Fig. 2B). AS for the gut injury, we observed villus shortening, epithelial cell loss, and mucosal wall thinning in vehicle treated mice following CLP, while 3-DZNeP -treated mice ameliorated these pathological changes (Fig. 2B). In the heart, although interstitial edema and focal necrosis could be seen in 3-DZNeP -treated mice, these changes were markedly improved when comparing with the vehicle treated CLP mice (Fig. 2B). These results show that blockage of EZH2 with 3-DZNeP reduces the pathological damages seen in multiple organs in response to severe sepsis, which likely improves the survival of septic mice.

3.3. 3-DZNeP lessens cytokine levels and bacterial burden in circulation and peritoneal fluid in septic mice

To evaluate the anti-inflammatory properties of 3-DZNeP, the levels of released cytokines were determined in the circulation and peritoneal fluid of septic mice. In coincidence with the findings of other labs and ours [14,16], CLP significantly increased the levels of TNF-α, IL-6, IFN-γ and IL-1β in the serum. These increases were attenuated by 3-DZNeP (Fig. 3A). The local peritoneal lavage inflammatory cytokines TNF-α, IL-6, IFN-γ and IL-1β expression exhibited a marked increase than those in the sham group, respectively. Consistent with observation of serum cytokine levels, 3-DZNeP attenuated the increases in TNF-α, IL-6, IFN-γ and IL-1β expression in peritoneal lavage fluid (Fig. 3B). Overall, these results indicate that the inflammatory response to sepsis in 3-DZNeP treatment mice is less vigorous than that in vehicle mice. Subsequently, the effect of pharmacological inhibition of EZH2 on bacterial burden was evaluated. It is noteworthy that bacterial burden in both systemic circulation and peritoneal fluid were significantly decreased in the 3-DZNeP treated mice compared with the vehicle mice (Fig. 3C).

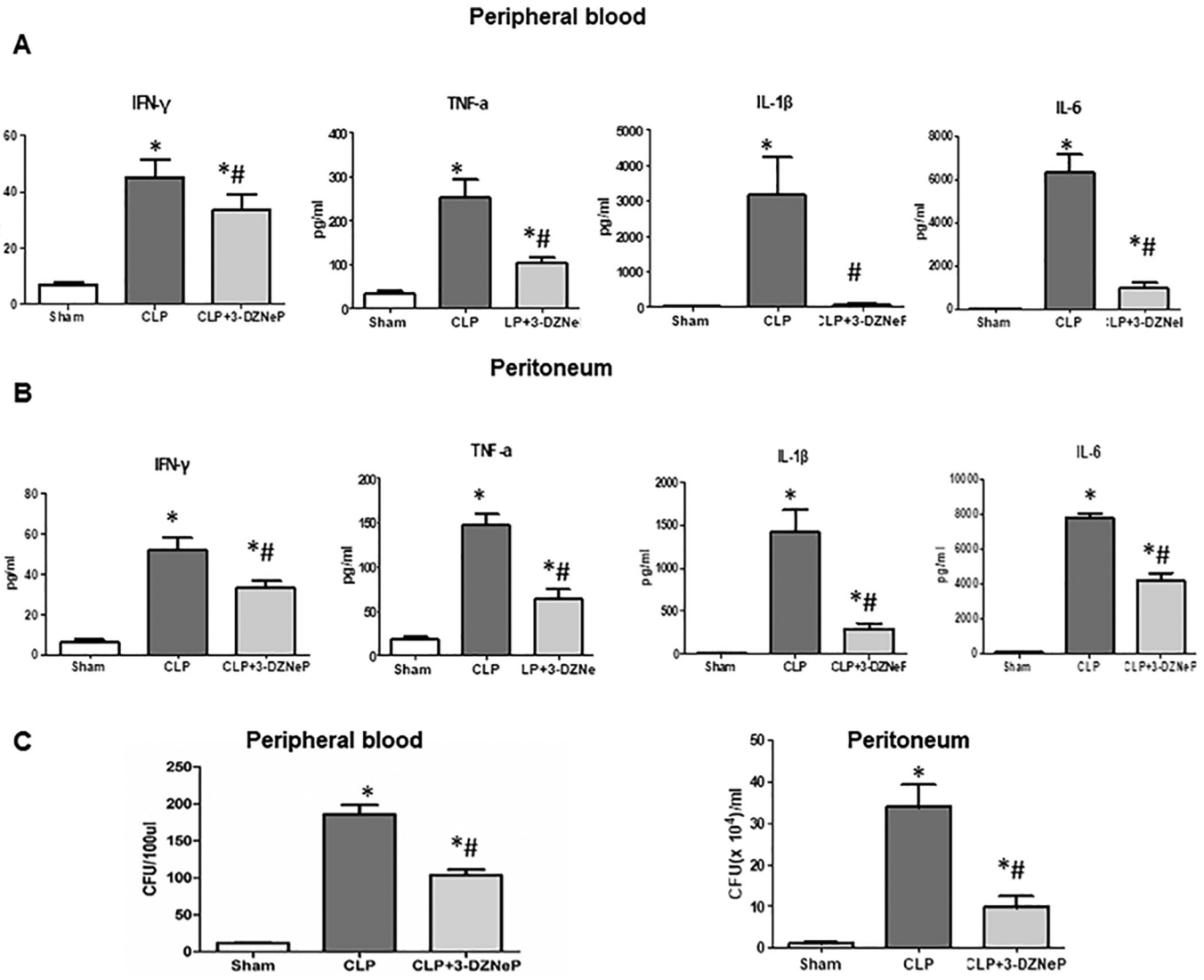

Fig. 3. 3-DZNep attenuates inflammatory cytokine levels and bacteria burden in peritoneal fluid and blood during sepsis. (A) Serum was collected 24 h after CLP and assayed for interleukin-6 (IL-6), tumor necrosis-α (TNF-α), IL-1β and interferon-γ(IFN-γ) levels by ELISA. (B) The peritoneal fluid was collected 24 h after CLP and assayed for IL-6, TNF-α, IL-1β and IFN-γ levels by ELISA. (C) Treatment with 3-DZNep significantly decreased the bacterial burden in the blood comparing with the vehicle treated mice have after CLP. Levels of aerobic bacteria are expressed as CFU per 100 μl for blood. The graphs depict data pooled from three independent studies showing similar results. (D) Treatment with 3-DZNep significantly decreased the bacterial burden in the peritoneum compared with the vehicle treated mice after CLP. Levels of aerobic bacteria are CFU per ml for peritoneal lavage. The graphs depict data pooled from three independent studies showing similar results. All data are expressed as mean ± SEM. (N = 12, $^{*}p < 0.05$ vs. control group, $^{\#}p < 0.05$ vs. vehicle treatment CLP mice, determined by one-way ANOVA for multiple group comparisons).

3.4. 3-DZNeP attenuates inflammatory cells activation on systemic blood circulation and promotes recruitment of macrophages while decreases migration of neutrophils into the infectious site of peritoneum

Prior studies and our reports have shown the activation of inflammatory immune cells following the onset of sepsis both in experimental mice and in critically ill patients [15,17]. Inasmuch, we attempted to determine whether 3-DZNeP affects the ratio of inflammatory cells in response to CLP. We found that the expression of EZH2 on the macrophages ($CD11b^{+}F4/80^{+}$) and neutrophils ($Gr1^{+}$) in the circulation were significantly increased at 24 h post CLP insult compared with sham mice (Fig. 4A, B). After treatment with 3-DZNeP, the percentage of both neutrophils and macrophages in the blood was significantly decreased in comparison with the vehicle treated CLP mice (Fig. 4A, B). Furthermore, the EZH2 expression on the neutrophils and macrophages were also significantly diminished with the administration of 3-DZNeP (Fig. 4A, B).

Macrophages and neutrophils are prominent bacteria-killing cells and constitute major cell populations in peritoneum when mice are subjected to CLP insult [15]. We next set out to investigate whether EZH2 play a novel role in regulating macrophage and neutrophil recruitment to peritoneum. We found that following CLP, both neutrophils and macrophages displayed a significant increase in $EZH2^{+}$ cells in the peritoneum 24 h post-CLP, when compared with sham mice (Fig. 4C). In coincidence with data from other labs [18], we also found that compared to mice subjected to sham surgery, CLP treated mice recruited more neutrophils but not macrophages into the peritoneum, which resulted in a significantly decreased macrophage: neutrophil ratio (Fig. 4D, E). Interestingly, the 3-DZNeP treated CLP mice manifested the opposite, which decreased the ratio of neutrophils but significantly promoted the macrophage recruitment into the peritoneum, therefore resulted in a significantly increased macrophage: neutrophil ratio in the infectious peritoneum (Fig. 4D, E). Putting together, EZH2 inhibition appears to alleviate sepsis induced neutrophil infiltration and

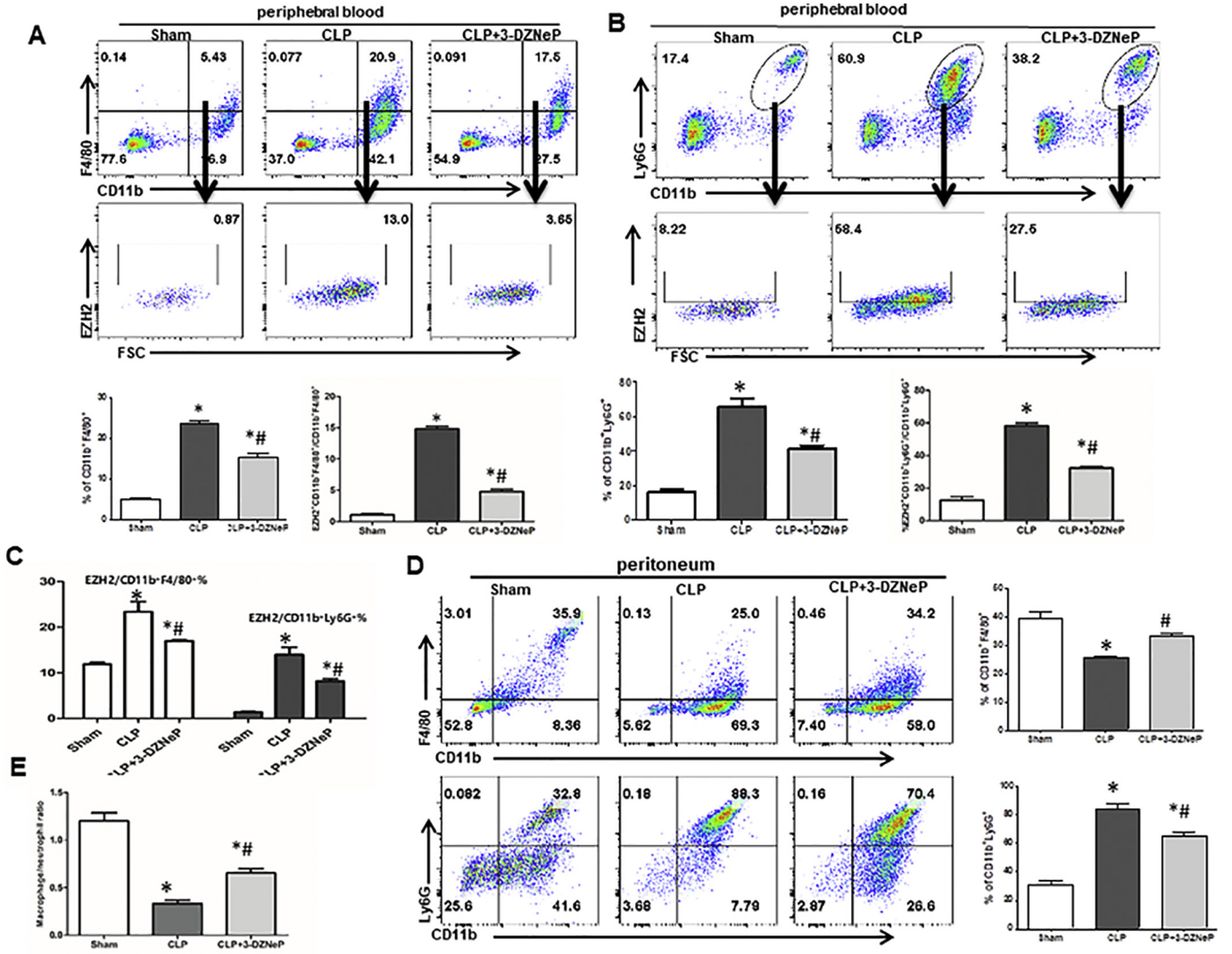

Fig. 4. 3-DZNep inhibits inflammatory cells activation on systemic blood circulation and affects neutrophils and macrophages recruitment into peritoneum. (A) The expression of EZH2 on macrophages (gated as $CD11b^+F4/80^+$) was assessed by flow cytometry 24 h after CLP insult. The percentage of macrophages (gated as $CD11b^+F4/80^+$) in the blood were also assessed in control and vehicle-treated and 3-DZNep treated groups. Representative dot plots are shown for expression of percentage EZH2 and its expression on the macrophages. (B) The expression of EZH2 on neutrophils (gated as $CD11b^+Ly6G^+$) was assessed by flow cytometry 24 h after CLP insult. The percentage of neutrophils (gated as $CD11b^+Ly6G^+$) in the blood was also assessed in control and vehicle-treated and 3-DZNep treated groups. Representative dot plots are shown for expression of percentage EZH2 and its expression on the neutrophils. (C) The expression of EZH2 on neutrophils (gated as $CD11b^+Ly6G^+$) and macrophages (gated as $CD11b^+F4/80^+$) in the peritoneum was assessed by flow cytometry 24 h after CLP insult in control, vehicle-treated and 3-DZNep treated groups. (D) The total percentage of neutrophils (gated as $CD11b^+Ly6G^+$) and macrophages (gated as $CD11b^+F4/80^+$) in the peritoneum was assessed by flow cytometry in control, vehicle-treated and 3-DZNep treated groups. Representative dot plots are shown for expression of percentage of neutrophils and macrophages. (E) The ratio of macrophages: neutrophils in the peritoneum was compared among the control, vehicle-treated and 3-DZNep treated groups. All data are expressed as mean ± SEM. (N = 12, $^*p < 0.05$ vs. control group, $^{\#}p < 0.05$ vs. vehicle treated CLP mice, determined by one-way ANOVA for multiple group comparisons).

macrophage recruitment in the circulation, and promotes the recruitment of macrophages but not neutrophils into the peritoneum in response to CLP-induced sepsis.

3.5. 3-DZNeP restores the percentage of phagocytotic cells in the bone marrow but not the spleen

Bone marrow is the critical organ in the production and maturation of phagocytes. We next set out to examine the potential effects of EZH2 inhibitor administration on the bone marrow cell population. As shown in Fig. 5A, there was a significantly decreased percentage of macrophages and neutrophils in the bone marrow 24 h after CLP in comparison with sham-operated mice. However, treatment with 3-DZNeP restored the macrophages and increased the percentage of neutrophils compared to vehicle-treated CLP mice. We further examined the phagocytotic cells in the spleen. Interestingly, there was a significant decreased ratio of neutrophils while no significant difference of macrophages in the spleen of CLP mice administered with 3-DZNeP compared to vehicle-treated CLP mice (Fig. 5B). Taken together, these data suggest that treatment with 3-DZNeP restores the macrophage population and increases the neutrophil composition in the bone marrow following CLP-induced sepsis.

3.6. 3-DZNeP reverses peritoneal macrophages' ability to engulf bacteria during sepsis

It is well known that severe sepsis often associates with the development of macrophage dysfunction [16], which is characterized by

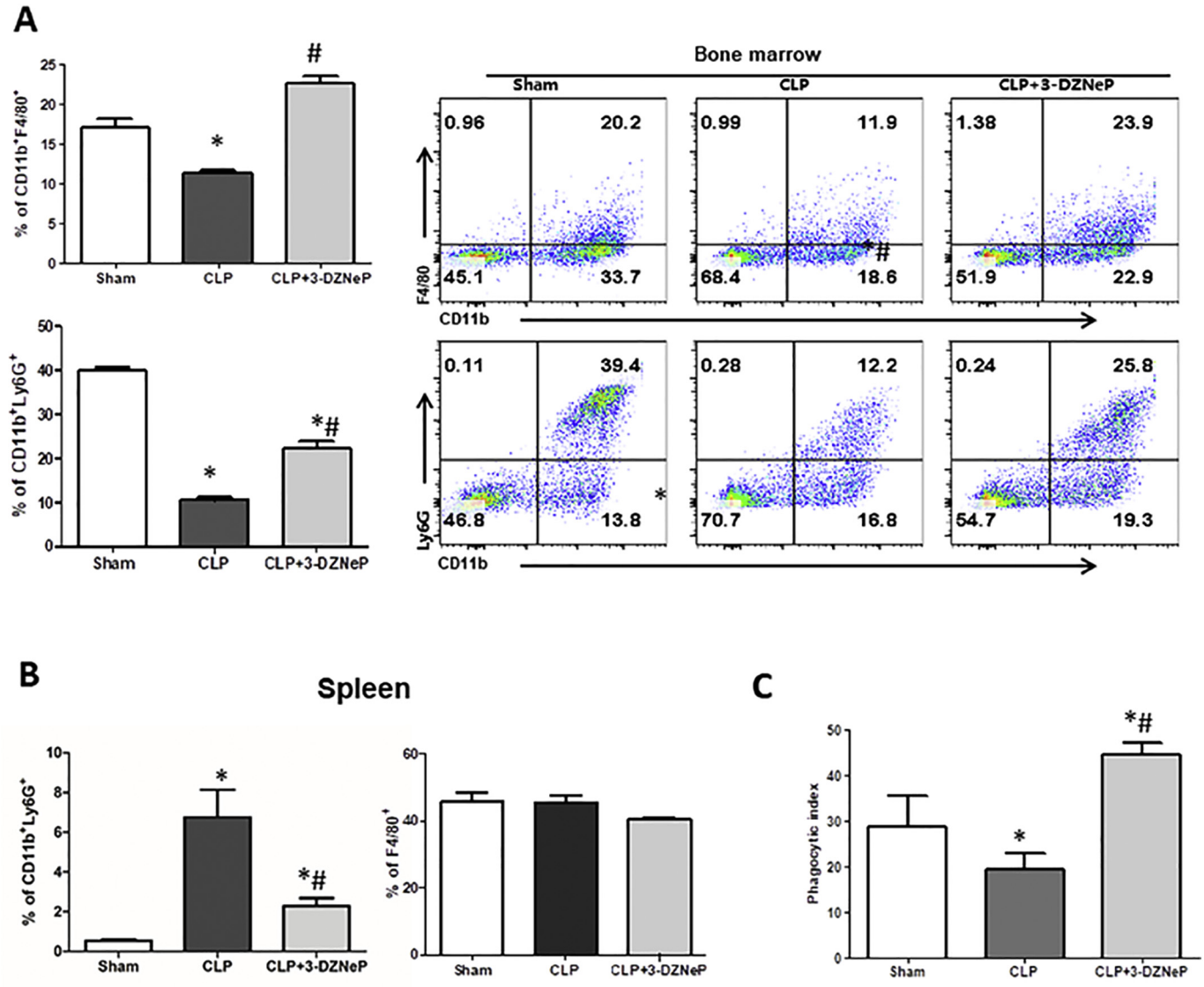

Fig. 5. 3-DZNep treatment restores the percentage of phagocytotic cells in the bone marrow not the spleen and retains peritoneal macrophages' ability to phagocytose bacteria during sepsis. The percentages of neutrophils (gated as $CD11b^+Gr1^+$) and macrophages (gated as $CD11b^+F4/80^+$) were quantified by flow cytometry from the bone marrow (A) and spleen (B) 24 h after surgery and compared among control and vehicle-treated and 3-DZNep treated groups. (C) Peritoneal macrophages were enriched by adhering to plastic plate and then fed with pHrodo- conjugated *E. coli*. The phagocytic capacity was measured by frequency of pHrodo fluorescence positive cells. Quantitative analyses of phagocytosis are compared among control, vehicle-treated and 3-DZNep treated groups. All data are expressed as mean ± SEM. (N = 12, $^*p < 0.05$ vs. control group, $^{\#}p < 0.05$ vs. vehicle treated CLP mice, determined by one-way ANOVA for multiple group comparisons).

reduced, even diminished ability to phagocytose bacteria. Thus, whether inhibition of EZH2 with 3-DZNeP affects this dysfunction during sepsis was assessed. Consistently, we found that peritoneal macrophages from septic mice exhibited a significantly declined capacity to phagocytose bacteria (Fig. 5C). In addition, 3-DZNeP treatment retained their ability of phagocytosis, resulting in a significantly higher phagocytic ability as compared to that from septic vehicle-treated CLP mice (Fig. 5C). These results show that inhibition of EZH2 contributes to reserving the diminished capacity of peritoneal macrophages to phagocytose bacteria during sepsis.

3.7. 3-DZNeP represses the lung injury during sepsis

Acute lung injury is one of the major adverse consequences of septic shock. In the preliminary study, we found that the mRNA expression of EZH2 and H3K27me3 in the lung tissues 24 h post CLP was significantly increased (data not shown). We next set out to use immunoblotting analysis to examine the effect of 3-DZNeP on the expression of EZH2 and H3K27me3 in the lung tissue 24 h after CLP insult. As shown in Fig. 6A, CLP induced a dramatic increase in the protein expression of pulmonary EZH2, which was accompanied by a marked increased level of H3K27me3. Administration of 3-DZNeP reduced the expression of EZH2 and also, significantly inhibited the increase of H3K27me3 in the lung tissue after sepsis. Therefore, we hypothesized that EZH2 inhibitor could have a role in mediating suppression of ALI. To address this hypothesis, indices of lung injury were measured in the lung 24 h after CLP. We observed that the vehicle-treated CLP mice exhibited an increased ALI parameters as indicated by a development of overt tissue edema and infiltration of neutrophils (Fig. 6B), a high lung wet/dry (W/D) ratio (Fig. 6C), and a marked pulmonary cell apoptosis exhibited by TUNEL staining (Fig. 6D) in comparison to sham control animals. However, the group with administering of 3-DZNeP had significantly reduced wet/dry ratio and also showed a marked reduction in the disruption of lung tissue architecture (Fig. 6B, C) in comparison with the vehicle-treated CLP mice. Furthermore, we found a significant decrease of apoptosis in the 3-DZNeP treated mice compared with vehicle-

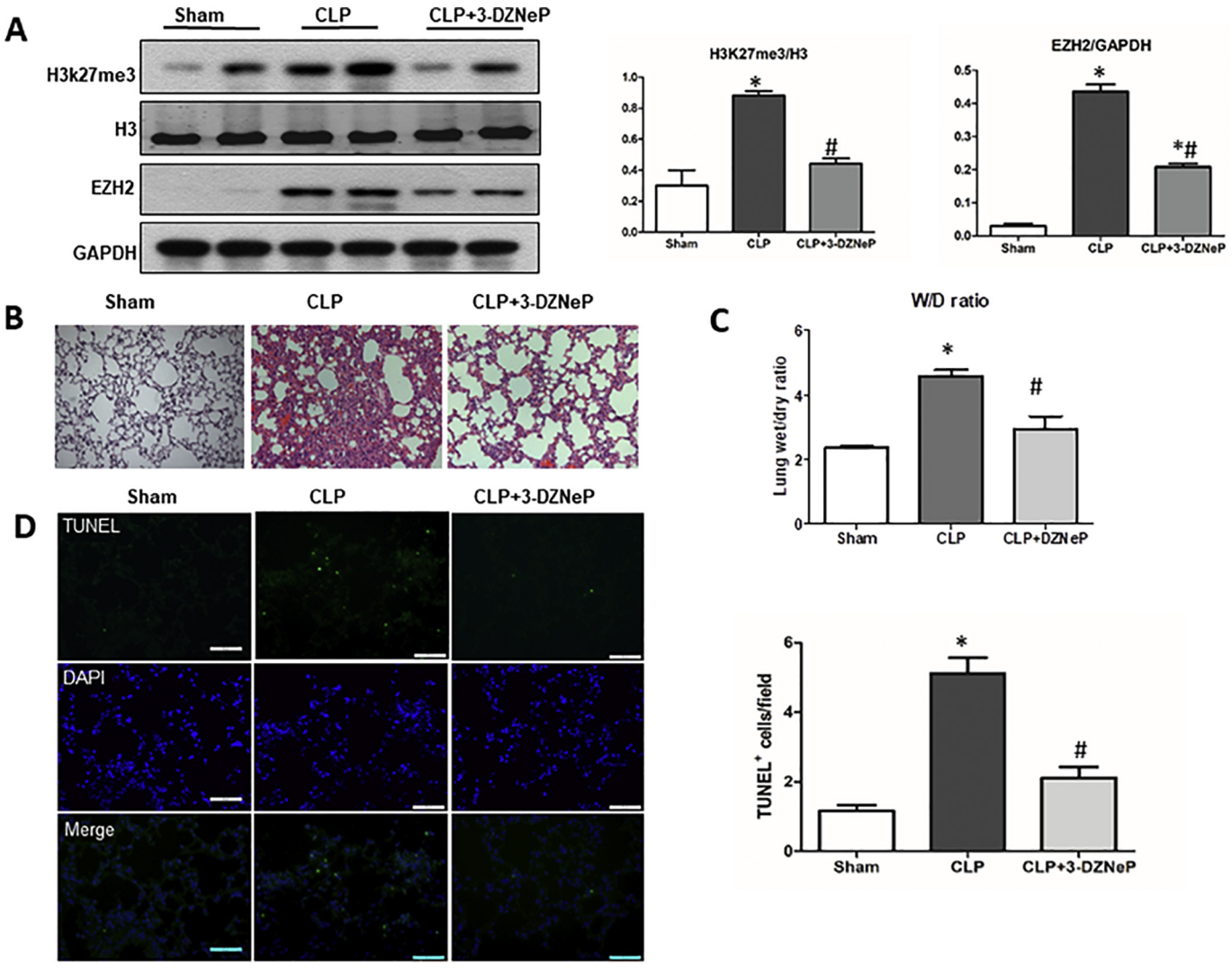

Fig. 6. 3-DZNep decreases the lung injury during sepsis. (A) Representative Western blot depicting whole lung tissue lysates probed for H3K27me3, H3, EZH2 and GAPDH from control, vehicle and 3-DZNep treated groups. Semi-quantitated by densitometry and expressed as integrated density (IDT) values of H3K27me3 relative to IDT values of H3, IDT values of EZH2 relative to IDT values of GAPDH. (B) Lungs were fixed, sectioned, and stained with H&E. Representative sections are shown from control, vehicle and 3-DZNep-treated groups. (Original magnification, ×200). (C) Evaluation of wet/dry weight ratio is compared among control, vehicle-treated and 3-DZNep treated groups. (D) Photomicrographs illustrate TdT-mediated dUTP nick-end labeling (TUNEL) staining of lung tissue collected at 24 h after surgery among control, vehicle-treated and 3-DZNep treated groups. Positive TUNEL staining cells were counted. All data are expressed as mean ± SEM. (N = 12, $^{*}p < 0.05$ vs. control group, $^{\#}p < 0.05$ vs. vehicle treated CLP mice, determined by one-way ANOVA for multiple group comparisons).

treated CLP mice (Fig. 6D). Putting together, these data suggest that administering of 3-DZNeP attenuates the injury after CLP-induced ALI.

3.8. 3-DZNeP alleviates inflammatory cytokines release and neutrophil infiltration during septic lung injury

Other studies and our prior reports have documented that the inflammatory cytokines play a pivotal role in the onset of ALI after sepsis [15,18]. Inasmuch, we observed that a significant upregulation of TNF-α, IL-6, IFN-γ, and IL-1β levels in the lung tissue homogenate of CLP mice. By contrast, the CLP mice administering with 3-DZNeP had significantly downregulated cytokine levels than vehicle treated mice, and these were similar to that of the sham surgery animals (Fig. 7A). Interestingly, IL-4 level was significantly deceased in the lung homogenate of the vehicle treated CLP mice compared to sham mice, while inhibition of EZH2 unregulated the IL-4 level (Fig. 7A).

Previous studies and our investigations have shown that inhibition of influx of neutrophils to the lung is central to repression of inflammation and injury after ALI. In the current study, we observed that neutrophil influx as measured by MPO activity (Fig. 7B), and $CD11b^{+}Ly6G^{+}$ neutrophils (Fig. 7C) was significantly reduced in the lung tissue of 3-DZNeP treated mice in comparison with vehicle-treated CLP mice. Furthermore, as our previous studies and others have shown that the most relevant chemokines for neutrophil recruitment into lungs were KC and MIP-2, it was interesting to note that the lung MIP-2, but not lung KC, was significantly decreased in 3-DZNeP treatment CLP mice when compared with vehicle-treated group (Fig. 7D). We further conducted immunostaining to address whether EZH2 was upregulated on the $Ly6G^{+}$ neutrophils in septic lung tissue. Interestingly, we observed an intense EZH2 labeling on the neutrophils (Ly6G positive) of lung tissue in vehicle treated CLP mice, by contrast, the 3-DZNeP treatment mice had significantly downregulated the positive EZH2 labeling on the $Ly6G^{+}$ neutrophils (Fig. 7E). These data suggest that administering of 3-DZNeP attenuates the pro-inflammatory cytokines release and neutrophil influx after CLP-induced ALI.

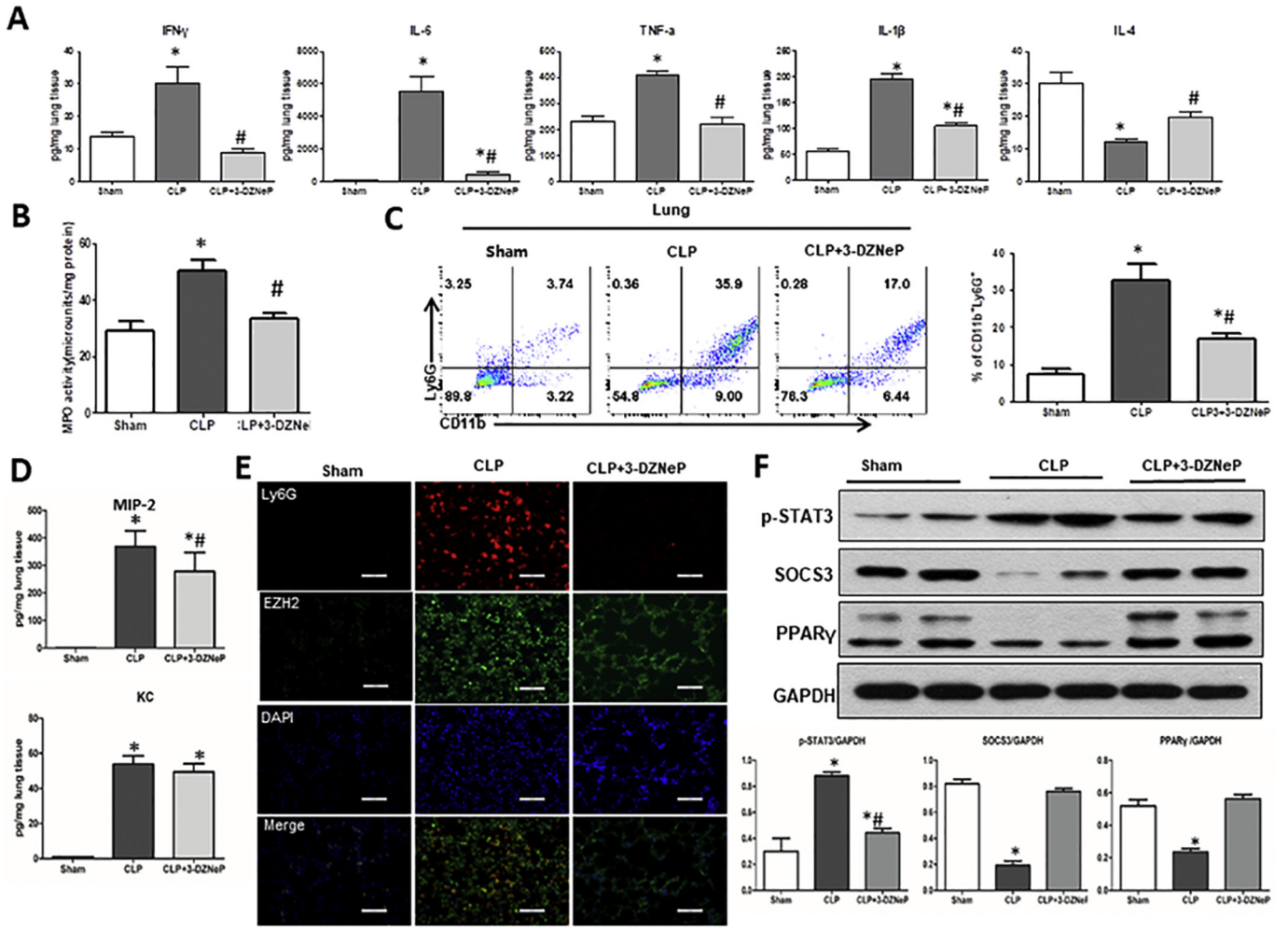

Fig. 7. 3-DZNeP protects mice from septic lung inflammation by suppressing STAT3 signaling pathway and activating Peroxisome Proliferator-Activated Receptorγ(PPARγ). (A) IFN-γ, IL-6, TNF-α, IL-1β1 and IL-4 levels in lung tissue were quantified by ELISA 24 h after surgery in control, vehicle-treatment and 3-DZNep treatment groups. (B) MPO activity was measured in lung homogenates 24 h after surgery in control, vehicle-treated and 3-DZNep treated groups. (C) Neutrophils were gated as $CD11b^{+}Ly6G^{+}$ cells in the lung tissue by flow cytometry 24 h after surgery in control, vehicle-treated and 3-DZNep treated groups. Representative dot plots are shown for percentage of neutrophils. (D) KC and MIP-2 levels in lung tissue were quantified by ELISA 24 h after surgery in control, vehicle-treated and 3-DZNep treated groups. (E) Representative images of double immunofluorescence staining for EZH2 and Ly6G in sections of lungs from control, vehicle-treated and 3-DZNep treated mice. (E) Representative western blot depicting whole lung tissue lysates probed for p-STAT3, SOCS3, PPARγ and GAPDH from control, vehicle and 3-DZNep treated groups. Semi-quantitated by densitometry and expressed as integrated density (IDT) values of p-STAT3, SOCS3, PPARγ relative to IDT values of GAPDH. (N = 12, $^{*}p < 0.05$ vs. control group, $^{\#}p < 0.05$ vs. vehicle treated CLP mice, determined by one-way ANOVA for multiple group comparisons). All data are expressed as mean ± SEM.

3.9. 3-DZNeP protects mice from septic lung inflammation by suppressing signal transducer and activator of transcription 3 (STAT3) signaling pathway and activating peroxisome proliferator-activated receptor γ (PPARγ)

We next set out to explore the underlying mechanism for the ability of EZH2 inhibitor to suppress the lung inflammation post sepsis. Recent studies have suggested that STAT3, a member of STAT family, is a major signaling molecule that regulates cytokine signaling in sepsis. Some researchers have shown that the inhibition of STAT3 phosphorylation is able to attenuate pulmonary inflammation and lung injury [19]. To evaluate whether EZH2 participates in ALI-associated STAT3 activation, we further examined the expression of phospho-STAT3 by immunoblot analysis. We found that the protein level of phosphorylated STAT3 was significantly increased in the lung homogenates of vehicle treated CLP mice, while this activation was significantly inhibited in the 3-DZNeP treated CLP mice (Fig. 7F). As previous reports have suggested that overexpression of suppressor of cytokine signaling-3 (SOCS3) may be protective in ALI and ARDS through suppression of STAT3 activation. We further evaluated the effect of 3-DZNeP on the expression of SOCS3 in septic lung tissue. Interestingly, we found that SOCS3 was significantly downregulated in the vehicle treated septic lungs (Fig. 7F). Of note, SOCS3 expression was markedly upregulated in the injured lung with 3-DZNeP administration (Fig. 7F).

It has been documented that PPARγ is the member of nuclear hormone receptor family and one of the isoforms of PPARs. PPARγ activation exerts anti-inflammatory and anti-apoptotic effects in many inflammatory diseases models including ALI [20]. In this study, we found that the expression of PPARγ was significantly decreased in the lung tissue post CLP insult, while 3-DZNeP administration dramatically increased PPARγ activity in lungs harvested from mice with ALI (Fig. 7F). Thus, our data indicate that blockade of EZH2 activity inhibits activation of STAT3 signaling pathway and activating the PPARγ in sepsis induced ALI.

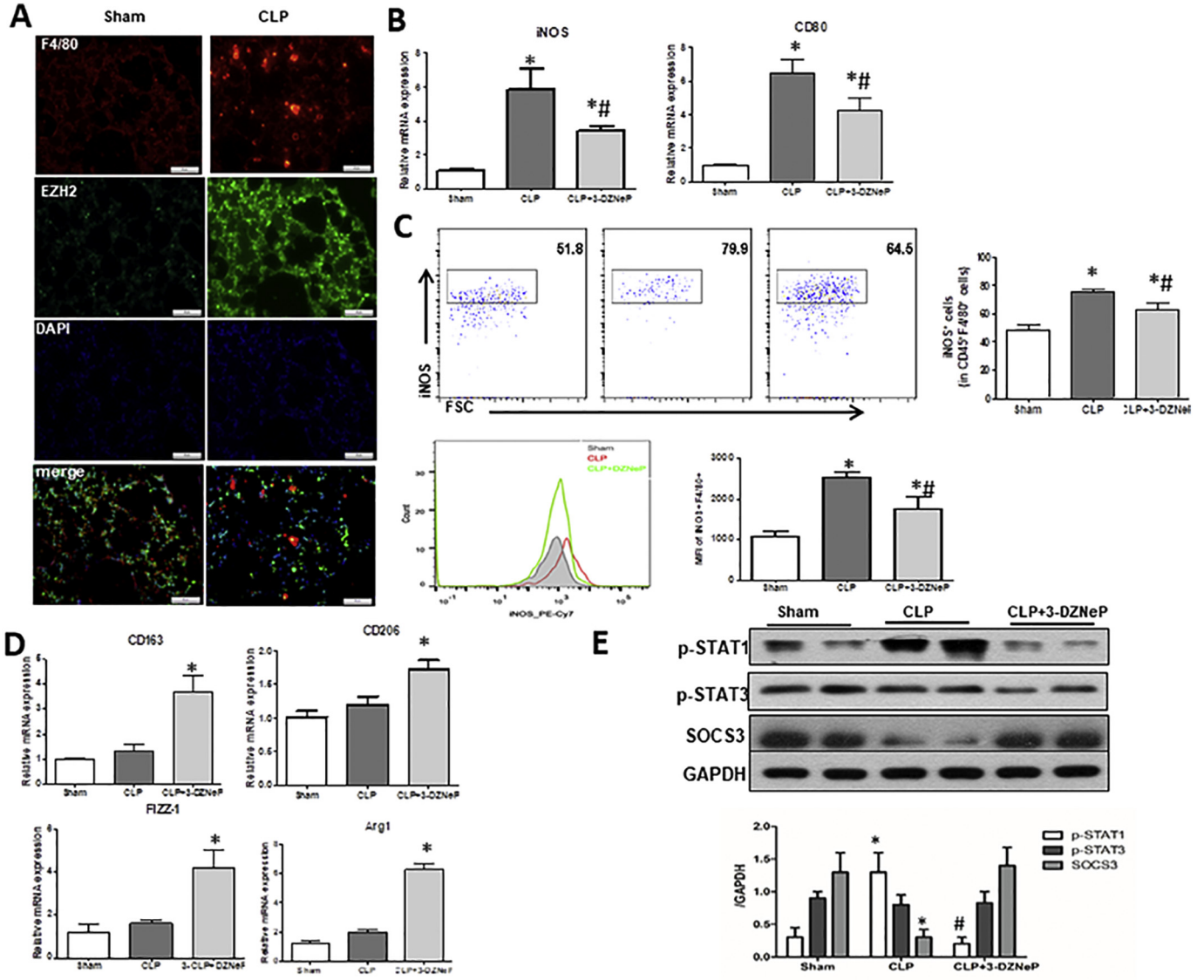

Fig. 8. 3-DZNeP induced resistance to septic lung injury is partially via blunting macrophage M1 polarization by regulating the SOCS3/STAT1 pathway. (A) Representative images of double immunofluorescence staining for EZH2 and Ly6G in sections of lungs from control and CLP mice. (B) The mRNA expression of INOS and CD80 was measured by quantitative PCR 24 h after surgery in control, vehicle-treatment and 3-DZNep treatment groups. (C) The ratio and concentration (MFI) of INOS on macrophages (gated as F4/80$^+$) in the lung homogenates was assessed by flow cytometry 24 h after CLP insult in control, vehicle-treated and 3-DZNep treated groups. (D) The mRNA expression of CD163, CD206, FIZZ-1 and Arg1 was measured by quantitative PCR 24 h after surgery in control, vehicle-treated and 3-DZNep treated groups. (E) Representative western blot depicting F4/80$^+$ macrophages from lung tissue probed for p-STAT1, p-STAT3, SOCS3 and GAPDH from control, vehicle and 3-DZNep treated groups. Semi-quantitated by densitometry and expressed as integrated density (IDT) values of p-STAT1, p-STAT3, SOCS3 relative to IDT values of GAPDH. (N = 12, $^*p < 0.05$ vs. control group, $^\#p < 0.05$ vs. vehicle treated CLP mice, determined by one-way ANOVA for multiple group comparisons). All data are expressed as mean ± SEM.

3.10. 3-DZNeP induced resistance to septic lung injury is partially via blunting macrophage M1 polarization

Currently, there is increasing evidence suggesting that macrophages are key factors in the pathogenesis of ALI/ARDS during sepsis. In our study, we found that expression of EZH2 on macrophages exhibited by double immunofluorescence staining for EZH2 and F4/80 in sections of lung tissue post-CLP (Fig. 8A). Macrophages have been shown to exhibit a spectrum of activated phenotypes, which can often be categorized under the M1/M2 paradigm. Emerging evidence suggests an important role for epigenetic mechanisms including DNA and histone modifications in modulating and transmitting signals during macrophage polarization and reprogramming. Inasmuch, we hypothesized that EZH2 may play a pivotal role in the modulation of macrophage polarization.

As there are two main polarization states of macrophages in the lung: the classically activated phenotype (M1) and the alternatively activated phenotype (M2), we investigated whether inhibition of EZH2 had a role in regulating the shift of macrophage phenotypes in the septic lungs. We found a significantly decreased mRNA expression of M1 markers [INOS(inducible nitric oxide synthase) and CD80] in the lung homogenates of 3-DZNeP treatment CLP mice in comparison with vehicle treated CLP mice (Fig. 8B). Flow cytometry assay was then used to sort F480$^+$ macrophagocyte and explore the iNOS production. As shown in Fig. 8C, both the ratio and the concentration (MFI) of iNOS$^+$F4/80$^+$macrophages (M1) in the lung homogenates 24 after CLP were significantly upregulated when compared with sham-operated mice. However, treatment with 3-DZNeP decreased the ratio and MFI of M1 macrophages (Fig. 8C). Interestingly, we did not find any difference in the mRNA expression of M2 markers (CD163, CD206, Arg1 and FIZZ-1) between the sham and vehicle treated CLP mice, while an increased

mRNA expression of M2 markers was noticed in the lung homogenates of 3-DZNeP treated CLP mice when compared with the vehicle treated CLP mice (Fig. 8D).

The shift of macrophage phenotypes is regulated by several signaling pathways. Previous studies have documented that SOCS3 and STAT1/3 are involved in the polarization of M1 macrophages with substantial crosstalk among these signaling pathways [21]. Specifically, SOCS3 negatively regulates the STAT1/3 activation and inhibits the M1 macrophages polarization. As 3-DZNeP showed the capacity in suppressing polarizing of M1-like macrophages in vivo, we hypothesized that this ability would be due to the regulation of SOCS3/STAT1/3 expression and/or function. Therefore, we further isolated monocytic cells from lung tissue and evaluated this signaling pathway. Compared with vehicle treated CLP mice, protein level of phos-STAT1 was significantly downregulated, while SOCS3 was upregulated in monocytes/macrophages sorted from septic lung tissue of 3-DZNeP administered mice (Fig. 8E). Interestingly, we did not observe any significant difference in phos-STAT3 expression among the sham, vehicle and 3-DZNeP treated mice.

4. Discussion

EZH2 plays critical roles in controlling a variety of cellular functions, including development and differentiation [10]. However, the contribution of EZH2 in the initiation and progression of sepsis and the underlying epigenetic mechanisms in macrophage activation are still unclear. In the current study, we found a marked upregulation of EZH2 and H3K27me3 levels both in septic patients and murine animal models. High level of EZH2 in the circulation, especially on $CD14^+$ monocytes, correlated with poor clinical outcome in septic patients. Pharmacologic inhibition of EZH2 with 3-DZNeP improved long-term survival by inhibiting the inflammatory cells activation and cytokines release in the circulation and infectious sites, and by promoting the bacteria clearance and replenishing the circulating monocyte and neutrophil pool from the bone marrow. Blockage of EZH2 also attenuated the progression of lung injury by reducing inflammatory cells infiltration and migration and decreasing the pulmonary cell apoptosis partially through activating the PPARγ and suppressing the STAT3 pathway. Furthermore, EZH2 inhibition reversed the macrophages dysfunction and inhibited phenotypic switch of macrophage to M1 polarization through SOCS3/STAT1 pathway. Thus, we identified EZH2 as an important epigenetic regulator of sepsis induced pro-inflammatory reaction and suggested that it could be a potential biomarker predicting clinical outcome and a new target for therapeutic interference in sepsis.

Previous studies have suggested that the inflammatory response in sepsis is regulated by histone methylation, including H3K4, H3K9 and H3K27 methylation [22]. To date, limited clinical research has focused on the epigenetic mechanisms of these diseases. Only recently, a study documented that the levels of histone methylation of peripheral WBCs were altered in critically ill patients. However, the clinical evidence concerning the role of EZH2 in sepsis is lacking. To our knowledge, we are the first to report that both the levels of EZH2 and H3K27me3 were significantly upregulated in the circulation of septic patients than controls. Also, patients who died maintained relative high level of EZH2 in the blood till Day 7 after diagnosis and high level of EZH2 on the $CD14^+$ macrophages in the beginning of the syndrome. These data indicate that the upregulation of EZH2 on the $CD14^+$ monocytes could affect the prognosis of septic patients. Until now, reliable biomarkers for predicting clinical outcomes among septic patients are still rare. Most recently, a first study of standardized multi-site flow cytometry was conducted to explore 47 leukocyte biomarkers for reliably discriminating which patients develop sepsis over the next 3 days, and found that only three of them (neutrophil and monocyte CD274 and CD279, together with monocyte HLA-DR) had the strongest association with clinical outcomes. Our study highlights a potential novel epigenetic biomarker for the early recognition and identification of patients who subsequently deteriorate clinically, which still needs large cohort study for confirmation in the future. In addition, we found that inhibition of EZH2 by a small molecular inhibitor 3-DZNeP significantly improved the long-term survival and lessened the multiple organ injury seen after sepsis. While this is only a small, single centered observational study, these results are comparable to the mouse results.

Excessive and uncontrolled inflammatory responses contribute to pathophysiological progress of sepsis. In the present study, CLP significantly increased the serum levels of IFN-γ, TNF-α, IL-1β and IL-6, which were attenuated by 3-DZNep. Moreover, 3-DZNep attenuated the increased expression of IFN-γ, IL-1β, TNF-α and IL-6 both in the peritoneal fluid and in the lung tissue in septic mice. This result suggests that 3-DZNep suppresses cytokine production at the transcriptional level.

Macrophages and neutrophils are efficient pathogen scavengers and the predominant source of inflammatory cytokines, making them critical effector cells against infection. In this study, we have discovered that pharmacological inhibition EZH2 with 3-DZNep diminished the macrophages and neutrophils activation on systemic blood circulation, and enhanced the recruitment of macrophages into the peritoneum of CLP mice, which may contribute to the improved bacterial clearance ability. Furthermore, we also found that treatment with 3-DZNep seemed to replenish the circulating monocyte and neutrophil pool from the bone marrow but not from the spleen, which may potentially enhance the host's ability to phagocytize foreign pathogens and eliminate bacteria from the circulation. These findings may partially explain the significantly better outcomes when treating 3-DZNep. Bone marrow is the critical organ in the production and maturation of lymphocytes and phagocytes [16]. The precise relationship between the EZH2 and bone marrow differentiation currently remains elusive. The inhibition of EZH2 may increase the percentages of macrophages and neutrophils through epigenetic modulation. Theoretically, EZH2 inhibitors may activate the gene promoters of bone marrow mesenchymal stem cells and facilitate their differentiation into macrophages and neutrophils, which needs future investigation.

Activation of STAT3 may be a common signaling mechanism that contributes to the pathogenesis of sepsis-induced ALI. Importantly, STAT3 activation in the lung occurs long before clinical signs of ALI are visible, suggesting that STAT3 plays an important role in early inflammatory responses which is related to production of the proinflammatory cytokines [19]. Our results showed that 3-DZNeP inhibited the phosphorylation of STAT3 in the lung tissues of septic mice. SOCS3. In addition, the JAK-STAT3 inducible protein, has been documented to regulate STAT3 activation via a negative feedback loop in macrophages [19,21]. Our data demonstrated that 3-DZNeP recovered the activation of SOCS3 which is consistent with a recent report showing that overexpression of SOCS3 may be protective in ALI and ARDS through suppression of STAT3 activation [19]. It also has been reported that PPARγ exhibits a cytoprotective effect against many inflammatory diseases including ALI [20]. In this study, we found that 3-DZNeP administration dramatically increased PPARγ activity in lungs harvested from CLP mice with ALI. Therefore, 3-DZNep treatment may attenuate inflammatory responses in the lung through modulating the SOCS3/STAT3 pathway and activating the PPARγ.

Macrophages are essential for the process of the inflammatory response in ALI/ARDS. In the acute phase of ALI/ARDS, resident alveolar macrophages tend to shift into the classically activated phenotype (M1) and release various potent proinflammatory mediators [21]. Although the mechanisms of macrophage activation have been extensively studied, the epigenetic regulation of the process is only beginning to emerge. Histone modifications are major regulators of macrophage functions. A previous investigation has reported that EZH2-mediated loss of let-7c determines inflammatory macrophage polarization via PAK1-dependent NF-kB activation in vitro. In our study, we further found that pharmacological inhibition of EZH2 with 3-DZNeP inhibited

the M1 polarization in vivo and had the tendency for the M2 polarization in the sepsis-induced ALI, which may partially explain the significantly resolution of inflammation that we have noted with 3-DZNep. We further found the beneficial effects of EZH2 inhibitor to suppress the M1 macrophages polarization in the septic lung by activating the SOCS3, thus suppressing the STAT1 but not STAT3 activation, which is consistent with the prior report documenting that myeloid specific SOCS3-deficient mice exhibited enhanced activities of STAT1/3 and increased plasma levels of proinflammatory cytokines and chemokines. Our results further indicate an essential regulatory role of EZH2 through the SOCS3/STAT1 pathway in the development of M1 macrophages in ALI/ARDS.

In conclusion, these data suggest that EZH2 could be a potential biomarker predicting clinical outcome and a new target for therapeutic interference in sepsis.

Author contributions

L. Tang, H. Sun, X. Zhou, S. Zhuang, Na. L and J. Bai designed the experiments and wrote the paper. D. Lv, H. Sun, X. Bao and H. Ren collected the clinical data and analyzed the data. Q. Zhang, X. Liu, Z Li and D Zhao conducted the experiments. X. Zhou provided advice and some reagents.

Declaration of competing interest

None.

Acknowledgments

This work was supported by grants from the National Natural Science Foundation of China (81500059 to L. Tang, 81670067 to J. Bai, 81670690 to Na L., 81670623 and 81830021 to S.Z.), the key program of Natural Science Foundation of Jiangxi Province (2018ACB 20016 to L. Tang), the Key Discipline Construction Project of Pudong Health Bureau of Shanghai (PWZxk2017-05 to N.L.), the Branch grant of National key grants of Ministry of Science and Technology of the People's Republic of China (2018YFA0108802 to S.Z.) and a grant from the Top-level Clinical Discipline Project of Shanghai Pudong.

References

[1] D.F. Gaieski, M. Goyal, What is sepsis? What is severe sepsis? What is septic shock? Searching for objective definitions among the winds of doctrines and wild theories, Expert Rev. Anti-Infect. Ther. 11 (9) (2013) 867–871.
[2] M. Ramanan, J. Myburgh, S. Finfer, R. Bellomo, B. Venkatesh, Publication of secondary analyses from randomized trials in critical care, N. Engl. J. Med. 375 (21) (2016) 2105–2106.
[3] F.I. Hassan, T. Didari, F. Khan, M. Mojtahedzadeh, M. Abdollahi, The role of epigenetic alterations involved in sepsis: an overview, Curr. Pharm. Des. 24 (24) (2018) 2862–2869.
[4] J. Thangavel, S. Samanta, S. Rajasingh, B. Barani, Y.T. Xuan, B. Dawn, J. Rajasingh, Epigenetic modifiers reduce inflammation and modulate macrophage phenotype during endotoxemia-induced acute lung injury, J. Cell Sci. 128 (16) (2015) 3094–3105.
[5] E.L. Greer, Y. Shi, Histone methylation: a dynamic mark in health, disease and inheritance, Nat. Rev. Genet. 13 (5) (2012) 343–357.
[6] A.J. Bannister, T. Kouzarides, Reversing histone methylation, Nature 436 (7054) (2005) 1103–1106.
[7] S.L. Foster, D.C. Hargreaves, R. Medzhitov, Gene-specific control of inflammation by TLR-induced chromatin modifications, Nature 447 (7147) (2007) 972–978.
[8] S. Chen, J. Ma, F. Wu, L.J. Xiong, H. Ma, W. Xu, R. Lv, X. Li, J. Villen, S.P. Gygi, X.S. Liu, Y. Shi, The histone H3 Lys 27 demethylase JMJD3 regulates gene expression by impacting transcriptional elongation, Genes Dev. 26 (12) (2012) 1364–1375.
[9] R. Margueron, D. Reinberg, The Polycomb complex PRC2 and its mark in life, Nature 469 (7330) (2011) 343–349.
[10] C. Lu, H.D. Han, L.S. Mangala, et al., Regulation of tumor angiogenesis by EZH2, Cancer Cell 18 (2) (2010) 185–197.
[11] L. Gan, Y. Yang, Q. Li, Y. Feng, T. Liu, W. Guo, Epigenetic regulation of cancer progression by EZH2: from biological insights to therapeutic potential, Biomark Res. 6 (10) (2018).
[12] H. Liu, Y. Liu, W. Liu, W. Zhang, J. Xu, EZH2-mediated loss of miR-622 determines CXCR4 activation in hepatocellular carcinoma, Nat. Commun. 6 (8494) (2015).
[13] Z. Yu, A. Rayile, X. Zhang, Y. Li, Q. Zhao, Ulinastatin protects against lipopolysaccharide-induced cardiac microvascular endothelial cell dysfunction via downregulation of lncRNA MALAT1 and EZH2 in sepsis, Int. J. Mol. Med. 39 (5) (2017) 1269–1276.
[14] L. Tang, J. Bai, C.S. Chung, J. Lomas-Neira, Y. Chen, X. Huang, A. Ayala, Programmed cell death receptor ligand 1 modulates the regulatory T cells' capacity to repress shock/sepsis-induced indirect acute lung injury by recruiting phosphatase SRC homology region 2 domain-containing phosphatase 1, Shock 43 (1) (2015) 47–54.
[15] J. Bai, L. Tang, J. Lomas-Neira, Y. Chen, K.R. McLeish, S.M. Uriarte, C.S. Chung, A. Ayala, TAT-SNAP-23 treatment inhibits the priming of neutrophil functions contributing to shock and/or sepsis-induced extra-pulmonary acute lung injury, Innate Immun. 21 (1) (2015) 42–54.
[16] S. Ono, H. Tsujimoto, S. Hiraki, S. Aosasa, Mechanisms of sepsis-induced immunosuppression and immunological modification therapies for sepsis, Ann. Gastroenterol. Surg. 2 (5) (2018) 351–358.
[17] A.C. Patera, A.M. Drewry, K. Chang, E.R. Beiter, D. Osborne, R.S. Hotchkiss, Frontline Science: defects in immune function in patients with sepsis are associated with PD-1 or PD-L1 expression and can be restored by antibodies targeting PD-1 or PD-L1, J. Leukoc. Biol. 100 (6) (2016) 1239–1254.
[18] A. Ayala, G.F. Elphick, Y.S. Kim, X. Huang, A. Carreira-Rosario, S.C. Santos, N.J. Shubin, Y. Chen, J. Reichner, C.S. Chung, Sepsis-induced potentiation of peritoneal macrophage migration is mitigated by programmed cell death receptor-1 gene deficiency, J. Innate Immun. 6 (3) (2014) 325–338.
[19] J. Zhao, H. Yu, Y. Liu, S.A. Gibson, Z. Yan, X. Xu, A. Gaggar, P.K. Li, C. Li, S. Wei, E.N. Benveniste, H. Qin, Protective effect of suppressing STAT3 activity in LPS-induced acute lung injury, Am. J. Physiol. Lung Cell Mol. Physiol. 311 (5) (2016) L868–L880.
[20] A. Li, Y. Liu, L. Zhai, L. Wang, Z. Lin, S. Wang, Activating peroxisome proliferator-activated receptors (PPARs): a new sight for chrysophanol to treat paraquat-induced lung injury, Inflammation 39 (2) (2016) 928–937.
[21] X. Huang, H. Xiu, S. Zhang, G. Zhang, The role of macrophages in the pathogenesis of ALI/ARDS, Mediat. Inflamm. 2018 (2018) 1264913.
[22] W. Zhang, H. Liu, W. Liu, Y. Liu, J. Xu, Polycomb-mediated loss of microRNA let-7c determines inflammatory macrophage polarization via PAK1-dependent NF-kappaB pathway, Cell Death Differ. 22 (2) (2015) 287–297.